

# Effect of oxygen defects on transport properties and $T_c$ of $\text{YBa}_2\text{Cu}_3\text{O}_{6+x}$ : Displacement energy for plane and chain oxygen and implications for irradiation-induced resistivity and $T_c$ suppression

Sergey K. Tolpygo, J.-Y. Lin, and Michael Gurvitch

*Department of Physics, State University of New York at Stony Brook, Stony Brook, New York 11794-3800*

S. Y. Hou and Julia M. Phillips\*

*AT&T Bell Laboratories, Murray Hill, New Jersey 07974*

(Received 9 August 1995; revised manuscript received 15 December 1995)

The effect of electron irradiation with energy from 20 to 120 keV on the resistivity, Hall coefficient, and superconducting critical temperature  $T_c$  of  $\text{YBa}_2\text{Cu}_3\text{O}_{6+x}$  thin films has been studied. The threshold energy of incident electrons for  $T_c$  suppression has been found, and the displacement energy for oxygen in  $\text{CuO}_2$  planes has been evaluated as 8.4 eV for irradiation along the  $c$  axis. The kinetics of production of the in-plane oxygen vacancies has been studied and found to be governed by athermal recombination of vacancy-interstitial pairs. The evaluated recombination volume constitutes about 21 unit cells. The increase in the  $T$ -linear resistivity slope and Hall coefficient at unchanged  $T_c$  was observed in irradiations with subthreshold incident energies and was ascribed to the effect of chain oxygen displacements. The upper limit on the displacement energy for chain oxygen has been estimated as 2.8 eV. In  $x=0.9$  samples the  $T_c$  suppression by in-plane oxygen defects and increase in residual resistivity have been found to be, respectively,  $-280$  K and  $1.5$  m $\Omega$  cm per defect in the unit cell. It is shown that  $T_c$  suppression by in-plane oxygen defects is a universal function of the transport impurity scattering rate and can be described qualitatively by pair-breaking theory for  $d$ -wave superconductors with nonmagnetic potential scatterers. Evaluation of scattering and pair-breaking rates as well as the scattering cross section and potential is given. A comparison of the influence of in-plane oxygen defects on transport properties with that of other in-plane defects, such as Zn and Ni substitutions for Cu, is also made. [S0163-1829(96)02718-x]

## I. INTRODUCTION

An enormous amount of work has been done on the study of defects and their effect on the transport, magnetic, and superconducting properties of high-temperature superconductors (HTS's).<sup>1</sup> It is believed that these studies may provide the key to understanding unusual normal-state properties and offer some insight into the mechanism of high- $T_c$  superconductivity. In the most thoroughly studied compound,  $\text{YBa}_2\text{Cu}_3\text{O}_{6+x}$  (YBCO), there can be basically two types of defects: in conducting  $\text{CuO}_2$  planes and in a "carrier reservoir" (CuO chain+BaO planes). Defects in the reservoir, such as oxygen vacancies and cation substitutions, directly influence carrier concentration in the planes and thus affect superconducting and normal properties mainly due to this influence. Defects in  $\text{CuO}_2$  planes act mainly as scattering centers. Since the planes are believed to be responsible for superconducting pairing, the influence of in-plane defects on transport properties may provide information on scattering and pairing mechanisms. For example, defect-induced  $T_c$  suppression can serve as a test for pairing symmetry in HTS's because nonmagnetic defects are pair breaking in anisotropic pairing superconductors, but have little effect on  $T_c$  in isotropic superconductors.

The most thoroughly studied in-plane defects in HTS's are defects on Cu sublattice such as Zn and Ni substitutions.<sup>1</sup> It is known that nominally nonmagnetic Zn impurities have a much stronger effect on  $T_c$  than nominally magnetic Ni, al-

though both have roughly the same effect on resistivity. Monthoux and Pines<sup>2</sup> (MP) have recently explained this fact by assuming that Zn impurities suppress spin fluctuations, which in their model mediate superconducting pairing of  $d$ -wave symmetry.<sup>3</sup> The effect of Ni impurities on  $T_c$  was shown to be consistent with the pair-breaking effect of purely potential scatterers.<sup>2</sup>

Since conducting planes comprise both Cu and O atoms, another type of defects that can be produced is the defect on oxygen sublattice such as oxygen vacancy or interstitial. The influence of these defects on superconducting and normal-state properties clearly presents a new avenue for study. This is because, first, current carriers have mainly  $p$  character (oxygen holes) and move preferably on oxygen sublattice and, second, both vacancies and interstitials carry charge in contrast to nominally neutral Zn and Ni impurities. Although oxygen defects were routinely produced in all the experiments involving high-energy particle irradiation of HTS's,<sup>4</sup> it was rather difficult to extract their effect from the gross influence of various atomic displacements which occurred. It was, however, established that  $T_c$  suppression at particle irradiation is proportional to the total nonionizing energy loss, i.e., to the concentration of displaced atoms.<sup>5</sup> More detailed study clearly requires a selective tool capable of producing only oxygen defects, e.g., low-energy electron irradiation.<sup>6-8</sup>

Electron irradiation has proven to be one of the best ways of creating uniformly distributed point defects in solids.<sup>9,10</sup>

For a solid, say, YBCO, displacements of atomic species on a sublattice  $i$  occur when the incident electron energy  $E$  exceeds a threshold energy  $E_c^i$ . The threshold is determined from a condition that the maximum energy transfer at an elastic electron-atom collision,  $E_m$ , become greater than the corresponding displacement energy,  $E_d^i$ , where

$$E_m = 2E(E + mc^2)/M_i c^2. \quad (1)$$

The defects formed due to such a knock-on process are known to be vacancy-interstitial pairs (Frenkel defects). These pairs are stable if the vacancy-interstitial separation exceeds some critical distance which depends on the material and type of crystal lattice. If  $E_d^i$  is known, the displacement cross section  $\sigma_d^i$  can be calculated, providing the basis for further evaluation of the concentration of defects  $n_d$  and quantitative analysis of defect-induced changes in transport and superconducting properties. Therefore, the displacement energy is a parameter of primary importance in many irradiation experiments. Although in most of the simple solids  $E_d^i$  lies in the range from 10 to 30 eV, it may vary greatly depending on the material, type of crystal lattice, and crystal lattice direction.<sup>9</sup> Despite these variations, due to the big difference in the atomic mass of atoms comprising YBCO, the lowest  $E_d^i$  should correspond to the lightest (oxygen) atoms. So it is easy to arrange a condition  $E_c^O < E < E_c^{Cu}$  ensuring that only displacements of oxygen will occur. The latter condition corresponds to  $E$  lower than some 300 keV. However,  $E_c^O$  has still to be evaluated, complicated by the existence of at least two oxygen sublattices, plane and chain.

There have been several attempts to determine  $E_d^O$  in HTS's, particularly in YBCO. Basu *et al.*<sup>11</sup> came up with  $E_c = 120$  keV corresponding to  $E_d^O = 18$  eV by observing a threshold energy for an  $e$ -beam-induced orthorhombic-to-tetragonal phase transition (see also Ref. 4). Since this value is typical for most of the simple oxides, the estimate of 18–20 eV has become widely used.<sup>4,5,7</sup> However, it seems clear that the ortho-tetra transition is governed by the chain oxygen content and, therefore, could be induced by oxygen loss under irradiation. If so, the  $E_c$  observed corresponds rather to the threshold for knock-on of chain oxygen into a microscope vacuum, which apparently requires higher energy than knock-on into an interstitial position. Another explanation is that the ortho-tetra transition under the beam was induced by a complete disordering of chain oxygen.<sup>11</sup> In any event, the experiment by Basu *et al.* does not tell us about oxygen displacements on  $CuO_2$  planes, which supposedly (at low concentration) have no effect on the crystal structure and are apparently invisible in a transmission electron microscope (TEM), but would rather dramatically affect carrier scattering and  $T_c$ .

On several occasions, we have reported about reproducible fabrication of Josephson weak links by lowering  $T_c$  in a narrow region across YBCO thin-film microbridges by a focused electron irradiation with energy as low as 60 keV and also about changes in the resistivity  $\rho$  even at 20-keV irradiation.<sup>12</sup> These results certainly implied that the  $E_d^O$  for both plane and, especially, chain oxygen is lower than 10 eV. Recently, combining low- $T$  electron irradiation with *in situ*  $T_c$  measurements, Legris *et al.*<sup>6</sup> evaluated  $E_d^O$ (planes) and  $E_d^{Cu}$  as 10 and 15 eV, respectively. The former value corre-

sponds to  $E_c = 80$  keV and still seems to be an overestimate because the experiments by Legris *et al.* were mostly done at high incident energies where the results are quite insensitive to the value of  $E_d^O$ . No attempt to determine  $E_d^O$ (chains) using methods different from those used in Refs. 4 and 11 (observation of changes in crystal lattice parameters, microstructure, and twin structure in TEM) has yet been undertaken.

Clearly, a straightforward method of evaluating  $E_d^O$  would be direct observation of the threshold in irradiation-induced changes in  $T_c$  and  $\rho$  as a function of  $E$ . Since, as we expect, this threshold lies below 80 keV, such an experiment requires thin films rather than single crystals in order to ensure uniform distribution of defects. Therefore, in this work we studied the effects of electron irradiation in the energy range from 20 to 120 keV on the transport and superconducting properties of high-quality YBCO thin films. Preliminary results have been reported in Ref. 8.

The paper is organized as follows. After a discussion of the experimental procedure (Sec. II), we give a detailed description of irradiation-induced changes in the resistivity and Hall coefficient (Sec. III A). The kinetics of defect production under electron irradiation is presented in Sec. III B. Then we present the evaluation of displacement energies for plane and chain oxygen (Secs. III C and III D). From the analysis of energy dependence of irradiation-induced change in  $T_c$  and residual resistivity, we show that  $E_d^O$ (plane) is  $8.4 \pm 0.4$  eV for the irradiation along the  $c$  axis. Analyzing the changes in the Hall coefficient and  $T$ -linear resistivity slope at irradiation with energies below the threshold for plane oxygen displacement, we estimate the upper limit on  $E_d^O$ (chain) as 2.8 eV. In Sec. IV we evaluate scattering and pair-breaking rates and discuss the pair-breaking mechanism of irradiation-induced  $T_c$  suppression. A comparison of oxygen in-plane defects with in-plane defects on Cu sublattice such as Zn and Ni substitutions is also given.

## II. EXPERIMENT

To ensure uniform distribution of irradiation-induced defects, 50-nm thin films were used. High-quality  $c_{\perp}$ -oriented  $YBa_2Cu_3O_{6+x}$  films were grown epitaxially on  $LaAlO_3$  substrates using the  $BaF_2$  process with subsequent full oxygenation ( $x \approx 0.9$ ). Details of the fabrication method, microstructure, and properties of the films have been published.<sup>13</sup> Using photolithography and liquid etching, the films were patterned into 10- $\mu$ m-wide and 40- $\mu$ m-long strips with four potential and two current leads (standard six-probe configuration) for resistivity and Hall measurements. A set of more than 40 samples has been studied. All of them were characterized by  $T_c$ ,  $\rho$  vs  $T$ , and  $R_H$  vs  $T$  (in a 5-T coil) before irradiation. These measurements have shown that the nonirradiated samples were nearly identical. Two types of irradiation experiments were performed. In the first type, a sample from the set was irradiated sequentially and the transport measurements were performed after each irradiation. In the second type, each sample was irradiated only once and an incremental irradiation dose was given to different samples of the set. The results were found to be consistent in both types of experiments. The irradiations were done at room temperature in a vacuum of a CM-12 Philips electron microscope, using

accelerating voltage from 20 to 120 kV. The beam current  $I$  was in the range from 3 to 50 nA. The substrate with the patterned film was attached to a brass sample holder using a silver glue to ensure good thermal contact; the film was grounded. Heating the samples under the beam was found to be negligible as verified by *in situ* resistivity measurements. In these measurements, the  $T$ -dependent resistivity of a sample (YBCO or Nb film of the same thickness and on the same substrate) served as a thermometer, thus providing the best possible estimate of the sample temperature. The electron beam was scanned with a constant rate over the pattern to accumulate the desired fluence  $\Phi = It/eA$ , where  $A$  is the scanned area (typically about  $20 \mu\text{m} \times 15 \mu\text{m}$ ),  $t$  is the irradiation time, and  $e$  is electron charge. The beam was perpendicular to the film surface, i.e., along the  $c$  axis of YBCO. The kinetics of accumulation of irradiation-induced defects was studied using *in situ* resistivity measurements during irradiation. To minimize the possible annealing of defects, the samples after irradiation were immediately placed into a variable-temperature He cryostat and the transport measurements were repeated. The recovery of  $T_c$ ,  $\rho$ , and  $R_H$  after irradiation was studied using anneals at 330 K in the He atmosphere of the cryostat, followed by the transport measurements.

Since it is known that irradiation of thin films which are produced and remain on substrates can give property changes which are related to strain in the film due to differences in the damage response between film and substrate,<sup>14</sup> we also studied the irradiation response of YBCO films grown on different substrates such as  $\text{LaAlO}_3$ ,  $\text{SrTiO}_3$ ,  $\text{NdGaO}_3$ , and Si buffered by YSZ. Also, films of different thickness ranging from 25 to 200 nm were used. Another potential source of error is a charging effect for a film on an insulating substrate; charging effects have been known to even produce film breakage in extreme cases, thus possibly contributing to an increase in resistivity. In order to eliminate this possibility, YBCO films grown on highly conducting doped Si substrates were also studied. In all cases the results obtained were found to be consistent with the set of data presented below. Also, special attention was paid to minimize surface contamination of the samples. No decomposition of films because of irradiation or sample degradation caused by surface contamination or oxygen loss in the microscope was observed in our irradiation experiments as verified by means of reversible annealing experiments and transport measurements.

### III. RESULTS

#### A. Transport properties

Irradiation causes  $T_c$  suppression and the appearance of the residual resistivity  $\rho_0$ , as shown in Fig. 1(a). The value of  $\rho_0$  was determined as a zero-temperature intercept of the linear extrapolation of  $T$ -linear resistivity curves. The increase in  $\rho_0$  definitely indicates that the irradiation produces oxygen defects in  $\text{CuO}_2$  planes. We intentionally present here the data for 80-keV irradiation at which neither the resistivity nor  $T_c$  would change if the oxygen displacement energy were 10 eV or higher. Radiation damage is not selective, however; i.e., with some probability the incident electrons may also displace oxygen on other sublattices because the

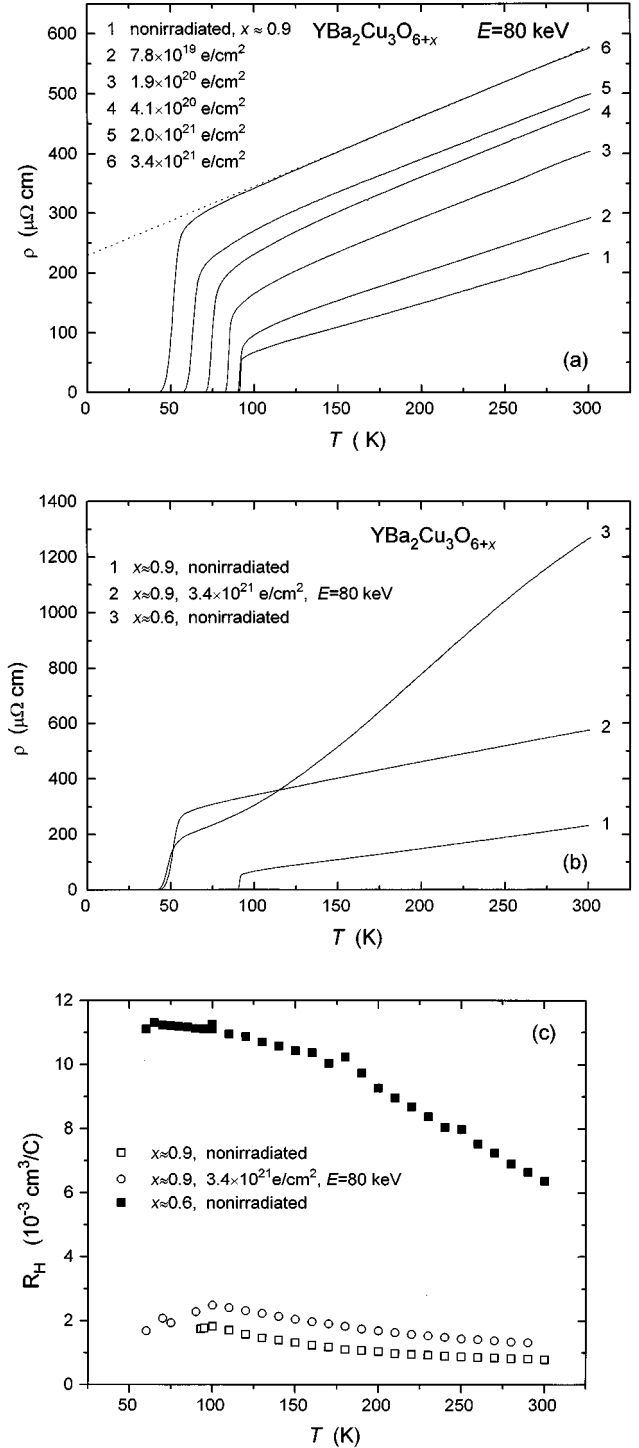


FIG. 1. In-plane ( $ab$ -averaged) resistivity  $\rho$  of  $\text{YBa}_2\text{Cu}_3\text{O}_{6+x}$  thin-film samples. (a)  $x \approx 0.9$  samples (made from one batch of film) after different doses of 80-keV electron irradiation; dotted line shows suggested residual resistivity  $\rho_0$  and  $T$ -linear resistivity slope  $\alpha$ ; (b) resistivity curves for the irradiated  $x \approx 0.9$  sample and for the nonirradiated oxygen-deficient sample ( $x \approx 0.6$ ) which has the same superconducting critical temperature; (c) Hall coefficient of the same samples as in (b).

displacement energy for these is likely to be the same or smaller than  $E_d^{\text{O}}(\text{plane})$ . In order to discriminate between the influence of oxygen defects on different sublattices, one can make use of the fact that oxygen defects in chains and BaO

planes should decrease the carrier concentration in planes,  $n$ , while the main effect of defects in  $\text{CuO}_2$  planes should be on carrier scattering. In order to show that the changes observed were not caused by a decrease in oxygen content in chains, we compared, first, the  $\rho$ -vs- $T$  curves of the irradiated sample and nonirradiated oxygen-deficient sample which has the same  $T_c$ . The oxygen-deficient sample was prepared by annealing the same film in He flow. The transport properties of these two samples are very different as shown in Fig. 1(b), indicating that the irradiation has nothing to do with chain oxygen removal. We arrive at the same conclusion when comparing the Hall coefficient data on these two samples [Fig. 1(c)]. It is seen that both the values of  $R_H$  and its temperature dependence in the irradiated fully oxygenated sample and in the nonirradiated oxygen-deficient sample (with the same  $T_c$ ) are totally different.

After annealing in a He atmosphere at slightly elevated temperatures (300–330 K),  $T_c$  and  $\rho$  of the irradiated samples recovered completely. This indicates that the overall oxygen content remained unchanged under irradiation; i.e., O atoms are displaced into interstitial positions rather than into the microscope vacuum.

In order to estimate the gross effect of all types of oxygen displacements on the carrier concentration, we looked, as a next step, at the slope  $\alpha = d\rho/dT$  in the  $T$ -linear region. There is a well-established correlation between  $\alpha$  and hole doping.<sup>15</sup> The origin of this correlation can be easily understood in a Drude model. While applicability of the Drude model and Boltzman transport theory to cuprates is actively debated (see, e.g., Ref. 16), we use this model from here on for the sake of simplicity and qualitative interpretations. So in the Drude model  $\rho = m^*/ne^2\tau_{tr}$ . The transport scattering rate in the temperature range of the  $T$ -linear resistivity can be expressed as  $1/\tau_{tr} = 1/\tau_{imp} + 2\pi\lambda_{tr}T$ , where  $\lambda_{tr}$  is the transport coupling constant and  $1/\tau_{imp}$  is the transport impurity scattering rate. Thus  $\alpha$  is proportional to  $\lambda_{tr}/n$ . Since the carrier-boson interaction constant  $\lambda_{tr}$  should only weakly depend on  $n$  due to the two-dimensional (2D) character of the quasiparticle spectrum, a change in  $\alpha$  would mainly reflect a change in the carrier concentration. Single-crystal data<sup>17</sup> indeed show a linear dependence of  $\alpha^{-1}$  on the carrier concentration or Drude spectral weight  $\omega_p^2$ . So, ideally, if  $n$  does not change at all, the slope of resistivity curves before and after irradiation should be the same. Figure 2 shows the normalized slope  $\alpha/\alpha_0$  for the irradiated samples, where  $\alpha_0$  is the resistivity slope before irradiation (the typical value of  $\alpha_0$  in the films studied is  $0.8 \mu\Omega \text{ cm K}^{-1}$ ). In order to compare the irradiation-induced changes in  $\alpha$  with changes in  $\alpha$  due to oxygen vacancies in chains, data are also shown for oxygen-deficient single crystals and laser-ablated thin films.<sup>17,18</sup> Here  $\alpha_0$  was taken as the resistivity slope in the optimally doped samples. The data for Zn-doped single crystals<sup>19</sup> are shown to represent the effect of in-plane defects on Cu sublattice (again,  $\alpha_0$  was taken as the slope in the undoped material). In oxygen-deficient samples, the  $T_c$ -vs- $\alpha$  dependence is similar to the  $T_c$ -vs- $x$  dependence and displays two plateaus, at 90 and 60 K. This is not the case in irradiated samples. Here  $T_c$  can be suppressed considerably (down to about  $T_{c0}/2$ ) at only slightly increased  $\alpha$ , similarly to what occurs at Zn doping. If we put the maximal irradiation-induced increase in  $\alpha$  into a correspondence with the change in  $\alpha$  observed at

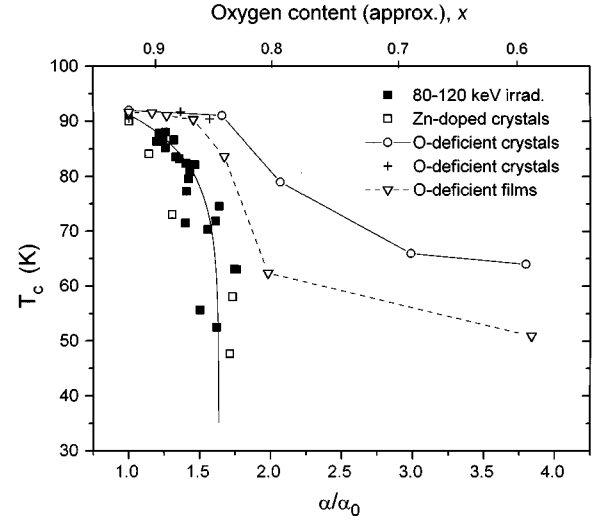


FIG. 2. Superconducting critical temperature (midpoint of resistive transitions) vs normalized  $T$ -linear resistivity slope for  $\text{YBa}_2\text{Cu}_3\text{O}_{6+x}$  ( $x \approx 0.9$ ) samples after electron irradiation. Data for oxygen-deficient single crystals and thin films were extracted from Ref. 17 ( $\circ$ ), Ref. 28 ( $+$ ), and Ref. 18 ( $\nabla$ ) and for  $\text{YBa}_2\text{Cu}_{3-y}\text{Zn}_y\text{O}_{7-\delta}$  single crystals from Ref. 19 ( $\square$ ). The upper scale shows the approximate oxygen content and corresponds only to nonirradiated single crystals. Lines drawn to guide the eye.

oxygen depletion, this change would imply a reduction in the oxygen content by less than 0.1 (from  $x \approx 0.93$  to  $x \approx 0.85$ ). Even if such a reduction occurred, it would have had a negligible effect on  $T_c$  as follows from the data in Fig. 2. We will discuss below that the likely cause of the increase in  $\alpha$  at irradiation is not the oxygen depletion, but rather oxygen disordering in chains, which occurs simultaneously with the production of in-plane defects, but is more pronounced at low doses due to a higher displacement cross section. In any event, the resistivity data suggest that the change in carrier concentration in irradiated samples is small and cannot be responsible for the observed  $T_c$  suppression.

Let us now turn to the Hall coefficient data on irradiated samples, shown in Fig. 3. Unfortunately, there is no simple

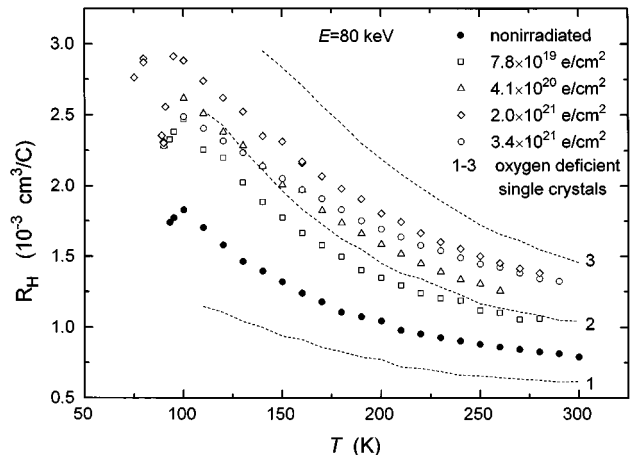


FIG. 3. Hall coefficient of  $\text{YBa}_2\text{Cu}_3\text{O}_{6+x}$  ( $x \approx 0.9$ ) thin-film samples [same as in Fig. 1(a)] after 80-keV electron irradiation; data for nonirradiated single crystals with  $x = 0.9$  (curve 1),  $x = 0.85$  (curve 2), and  $x = 0.78$  (curve 3) were taken from Ref. 17.

relation (such as  $R_H \propto 1/n$  in semiconductors) between the Hall coefficient and carrier concentration in HTS's because the former is strongly temperature dependent and the cause of this temperature dependence is not completely understood. However, qualitative information can be obtained comparing the data on irradiated samples with that on oxygen-deficient ones for which the correlation of the Hall coefficient and its  $T$  dependence with oxygen content and carrier concentration have been studied.<sup>17,18,20,21</sup> It is seen that at small doses there is about 25% initial increase in the Hall coefficient of irradiated samples, which correlates with the increase in  $\alpha$  occurring in the same dose range. A further 50-time increase in the irradiation dose results in about the same or even smaller changes. The temperature dependence of  $R_H$  in irradiated samples remains nearly unchanged. A comparable increase in the Hall coefficient is also observed in Zn-doped YBCO single crystals.<sup>19,22</sup> We would like to note that the increase in  $R_H$  not necessarily signifies the decrease in carrier concentration, but can result from an interplay of inelastic and elastic scattering. It was argued that a better representation of the carrier concentrations is provided by the slope of  $\cot \Theta_H$  (inverse Hall mobility) vs  $T^2$ , where  $\Theta_H$  is the Hall angle.<sup>19,21</sup> A detailed analysis of the Hall angle in the irradiated samples requires more space and will be presented elsewhere. Note only that its slope indeed remains practically unchanged after irradiation in agreement with observations by Legris *et al.* and data on Zn-doped YBCO. For the purposes of this paper, it is sufficient that all the  $R_H(T)$  curves for the irradiated samples (with  $T_c$  ranging from 91 down to 50 K) lie around the  $R_H$ -vs- $T$  curve for  $x=0.85$  nonirradiated single crystals ( $T_c \approx 91$  K). The Hall coefficient of the sample receiving the highest dose used in this study ( $T_c \approx 50$  K) is certainly smaller (at all temperatures) than that of the nonirradiated single crystal with  $x=0.78$  ( $T_c \approx 84$  K). This suggests that the decrease in carrier concentration, if any, due to the integral effect of all oxygen displacements on different sublattices is not the case of the observed  $T_c$  suppression in irradiated samples.

All the observations above, though indirect, unambiguously show that the prime cause of both irradiation-induced  $T_c$  suppression and residual resistivity is oxygen defects on  $\text{CuO}_2$  planes. This enables the determination of the displacement energy for in-plane oxygen by studying the changes in  $T_c$  at different energies of incident electrons.

### B. Kinetics of defect production

In a dilute (small concentration of defects) limit, one would expect the changes in  $\rho_0$  to be proportional to the concentration of in-plane defects. Substitution studies<sup>1</sup> as well as irradiation experiments show<sup>5,23</sup> that the changes in  $T_c$  are indeed proportional to the concentration of in-plane defects. When  $E_m$  does not exceed  $E_d$  by much, as in our case, the energy of the primary knocked-on atom is not sufficient to cause secondary displacements. Then, making a standard assumption that the probability of defect formation is one at  $E \geq E_d^0$  and zero at  $E < E_d^0$ ,  $\sigma_d$  can be obtained by integrating the Mott-Rutherford differential cross section from  $E_d^0$  to  $E_m$ . This gives (see, e.g., Ref. 10)

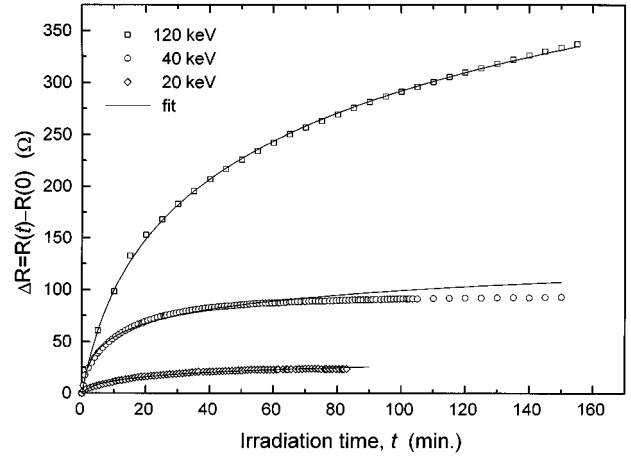


FIG. 4. Change in the room-temperature resistance of  $\sim 4\text{-}\mu\text{m}$ -long and  $3\text{-}\mu\text{m}$ -wide thin YBCO film microbridges during electron irradiation. Beam current is approximately the same at different energies. Solid lines are fits to the athermal model, Eq. (4)+Eq. (6b).

$$\sigma_d = \frac{\pi Z^2}{\beta^2 \gamma^4} \left( \frac{e^2}{mc^2} \right)^2 \left( \frac{E_m}{E_d^0} - 1 - \beta^2 \ln \frac{E_m}{E_d^0} + \pi \alpha \beta \left\{ 2 \left[ \left( \frac{E_m}{E_d^0} \right)^{1/2} - 1 \right] - \ln \frac{E_m}{E_d^0} \right\} \right), \quad (2)$$

where  $\beta = V/c$  ( $V$  is the speed of electrons;  $c$  is the speed of light),  $1/\gamma = 1 - \beta^2$ , and  $\alpha = Z/137$  ( $Z=8$  for oxygen). The number of displacements per oxygen atom (DPA) is given by  $N_d = \sigma_d \Phi$ . So, at low doses,  $T_c$  and  $\rho_0$  should be linear functions of  $\Phi$ . Correspondingly, the dependence of  $dT_c/d\Phi$  and/or  $d\rho_0/d\Phi$  on incident electron energy should be determined by  $\sigma_d(E)$ . However, first, the criterion of a small dose has yet to be established. And, second, this simple consideration can in reality be complicated by recombination and aggregation of defects as well as by their migration to the ‘‘sinks’’ (dislocations, grain boundaries, etc.), all of which reduce the concentration of remaining point defects.

In order to establish the kinetics of the accumulation of defects, we performed *in situ* resistance measurements during electron irradiation. Typical results are shown in Fig. 4. The important features found in these measurements are as follows. First, the accumulation kinetics is highly nonlinear even at nominally small ( $N_d \ll 1$ ) doses as if the defect production has a strong tendency to saturation. The implied saturation level depends not only on the incident electron energy, but also on the beam current. Second, the irradiation effect on resistivity decreases strongly with decreasing energy, indicating an approach to the threshold. However, electrons with energy as low as 20 keV are still capable of producing noticeable changes in the room-temperature resistivity of YBCO.

Figure 5 shows the  $T_c$ -vs- $\Phi$  dependence at  $E=80$  keV and clearly demonstrates nonlinear behavior which resembles a tendency to saturation at high fluences. Analysis of the data in Figs. 4 and 5 shows that the observed kinetics cannot be explained by a first-order back reaction with time constant  $\tau$  (diffusion-controlled recombination of defects). Also, a detailed study of the kinetics of recovery after irra-

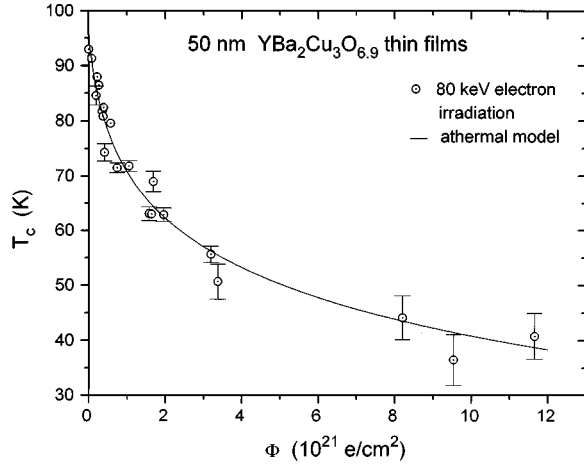


FIG. 5. Critical temperature of the irradiated samples (midpoint of resistive transition) vs irradiation fluence of 80-keV electron irradiation. Error bars denote the width of superconducting transitions (90%–10% level) in cases where this width exceeds the size of the data points. The solid line is the best fit to the athermal model, Eq. (4)+Eq. (6a), with fitting parameters  $\delta T_c = 280 \pm 30$  K per defect cell<sup>-1</sup>,  $v_r = 21 \pm 2$ .

diation shows that it is neither a first- nor second-order back reaction. We have found a stretched exponential relaxation kinetics  $\exp(-t/\tau)^\beta$  with  $\beta \approx 0.43$ , which holds from the very early stages of the recovery process.<sup>8,24</sup>

The mentioned features of the defect accumulation are similar to those found in irradiation experiments with simple metals<sup>25</sup> and complex solids,<sup>14</sup> and studied in detail, e.g., for alkali halides.<sup>26</sup> Pooley (see references in Ref. 26) proposed that the prime cause of the nonlinear accumulation kinetics is the athermal interstitial-vacancy recombination. The idea is that if an interstitial and vacancy are formed within some critical distance, they will spontaneously recombine and this process does not require any activation energy. The recombination is thus not governed by random diffusion and cannot be regarded as a back reaction in the normally accepted sense. The critical distance can be represented by assuming a recombination (“trapping”) volume  $V_r$  around a defect. If a newly formed interstitial falls within such a volume belonging to an existing vacancy, the two will recombine and no new vacancy will result from the displacement event. At room temperature, the interstitials diffuse rapidly to sinks and, therefore, can be ignored in the subsequent damage process, provided they are not initially formed within the trapping volume. Using these assumptions, Hughes and Pooley<sup>26</sup> solved the athermal model exactly and found the following time dependence of the vacancy concentration:

$$n_v = (1/V_r) \ln(V_r F t + 1), \quad (3)$$

where  $F$  is the basic rate of defect production per unit volume. Since  $F = N_O N_d / V_{\text{cell}}$  and  $n_v = N_v / V_{\text{cell}}$ , Eq. (3) transforms into

$$N_v = \frac{1}{v_r} \ln(v_r N_O \sigma_d \Phi + 1), \quad (4)$$

where  $N_v$  is the number of vacancies per unit cell,  $N_O$  is the number of oxygen atoms in the unit cell which can be displaced,  $V_{\text{cell}}$  is the unit cell volume, and  $v_r = V_r / V_{\text{cell}}$ . In a low-dose limit

$$v_r N_O \sigma_d \Phi \ll 1, \quad (5)$$

Eq. (4) reduces to the standard expression  $N_v = N_O \sigma_d \Phi$ . Hereafter we use  $N_O = 4$  since only displacements of plane oxygen are of interest.

We assume that the main contribution to the changes in resistivity and  $T_c$  of irradiated samples is due to in-plane oxygen vacancies since they definitely lie on conducting planes. The oxygen atoms are displaced into interstitial positions which are probably far from the planes and thus have less influence. Also, at room temperature the interstitials are mobile, can aggregate, and diffuse to sinks, and so the concentration of interstitials after room-temperature irradiation should be smaller than the concentration of vacancies. Therefore, in the following analysis we completely disregard the possible contribution of interstitials. We would also like to emphasize that the processes of radiation defect formation and recombination is complex. As a result, even in simple monoatomic solids the experimental determination, or calculation from first principles, of the exact defect concentration is extremely difficult (for a discussion see Refs. 9, 25) and often can only be done by comparing relative numbers as well as results of calculations and experiments on defect-induced changes in different physical properties. Therefore, in this and the following sections we will use the simplest model which we believe, nevertheless, catches the essential physics and provides accurate estimates of induced defect concentrations in such complex solids as HTS's.

In order to compare the data in Figs. 4 and 5 with the prediction of the athermal model, we use the linear relations which should be valid at a low concentration of defects,

$$T_c(\Phi) = T_c(0) - \delta T_c N_v, \quad (6a)$$

$$\rho(\Phi) = \rho(0) + \delta \rho N_v, \quad (6b)$$

with  $N_v$  given by (4) and  $\Phi \propto t$ . Here  $\delta T_c$  and  $\delta \rho$  are parameters characterizing the single-defect contribution. The fits to Eqs. (6) are shown as solid lines. The fitting by the athermal model was found to be unique in the sense that from a number of other possible dependences considered (such as first- and second-order back reactions, stretched exponentials, etc.) neither fits the data as well as Eq. (6) with only two fitting parameters ( $v_r$  and either  $\delta T_c$  or  $\delta \rho$ ).

We have found  $E_d^O$  for plane oxygen to be 8.4 eV (details of the evaluation are given below). At  $E = 80$  keV,  $\sigma_d$  is then  $6.09 \times 10^{-23}$  cm<sup>2</sup>, and the best fit to the data in Fig. 5 gives  $v_r = 21 \pm 2$ , which corresponds to the trapping volume containing about 150 oxygen sites and critical distance  $\sim 3$  unit cell lengths: very reasonable figures. For a comparison, the recombination volume usually contains  $\sim 100$  sites in simple metals<sup>9,25</sup> and about 3000 halogen sites in alkali halides.<sup>26</sup>

### C. Displacement energy for oxygen on planes

Now we turn to the evaluation of displacement energy for oxygen on CuO<sub>2</sub> planes. A straightforward way of doing this is to use slopes  $dT_c/d\Phi$  and/or  $d\rho/d\Phi$  measured in the

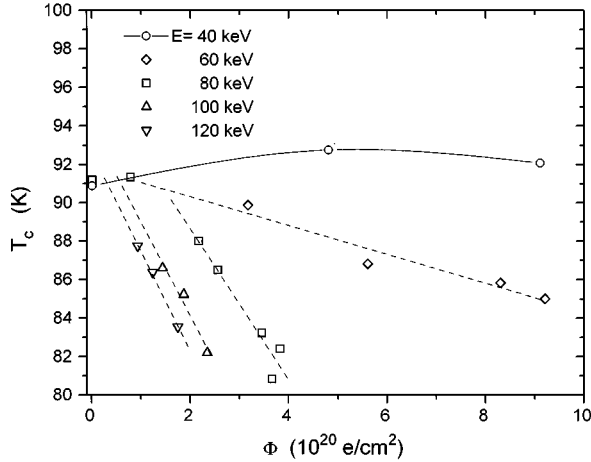


FIG. 6.  $T_c$ -vs-irradiation fluence at different energies of incident electrons. Dashed lines are fits to a  $\Phi$ -linear dependence.

low-dose limit (5) [where they reduce to  $4\sigma_d(E)\delta T_c$  and  $4\sigma_d(E)\delta\rho_0$ , respectively] and fit them to the energy dependence of  $\sigma_d$  according to Eq. (2).<sup>6</sup> This requires measurements at  $\Phi \ll 10^{20} e/cm^2$ . However, at such low doses additional complications arise. We found that at a displacement of only chain oxygen  $T_c$  increases by 2–3 K (from 91 to 93.5 K).<sup>27</sup> This increase resembles the increase in  $T_c$  of single crystals and epitaxial films at oxygen depletion, sometimes observed within the 90-K plateau region.<sup>18,28,29</sup> By contrast, in-plane oxygen displacements only suppress  $T_c$ . Since both types of displacements are produced simultaneously, a superposition of these two dependences results in, depending on  $E$ , either a plateau or small maximum in  $T_c$ -vs- $\Phi$  dependence at low doses. Therefore, the measurements of  $T_c$  suppression have to be performed outside this region and, as a consequence, at higher doses than those required by the condition (5).

$T_c$ -vs- $\Phi$  dependences beyond the described region are shown in Fig. 6. The existence of the threshold incident energy for  $T_c$  suppression slightly below 60 keV is obvious from the data. In the small range of  $\Phi$  shown ( $\Phi < 6 \times 10^{20} e/cm^2$ ), we can approximate  $T_c$  vs  $\Phi$  by a linear dependence, keeping in mind that its slope ( $\Delta T_c/\Delta\Phi$ ) is somewhat smaller than in the true low-dose limit. The same procedure was applied to  $\rho_0$ -vs- $\Phi$  dependences at different energies. We fitted both slopes to the  $E$  dependence of displacement cross section (2) with  $E_d^O$  being the only fitting parameter, as shown in Fig. 7. The best fit to the data gives  $E_d^O = 8.4 \pm 0.4$  eV, corresponding to  $E_c \approx 58$  keV.

The evaluated  $E_d^O$  is considerably lower than the widely used estimate ( $\sim 20$  eV) and lower than the value found by Legris *et al.*<sup>6</sup> We would like to stress here that thermal recombination (annealing) of defects (irradiations were done at room temperature) cannot result in an apparent reduction of the  $E_c$ , quite the opposite. The stability of Frenkel defects depends on the vacancy-interstitial separation, which increases with increasing energy transfer  $E_m$ . Therefore, faster annealing of defects produced at lower  $E$  would mimic a shift of  $E_c$  toward higher energies. So the actual  $E_d^O$  may only be slightly lower than we evaluated.

Experiments with thicker films (up to 200 nm) prepared by the BaF<sub>2</sub> method and by laser ablation verified that the

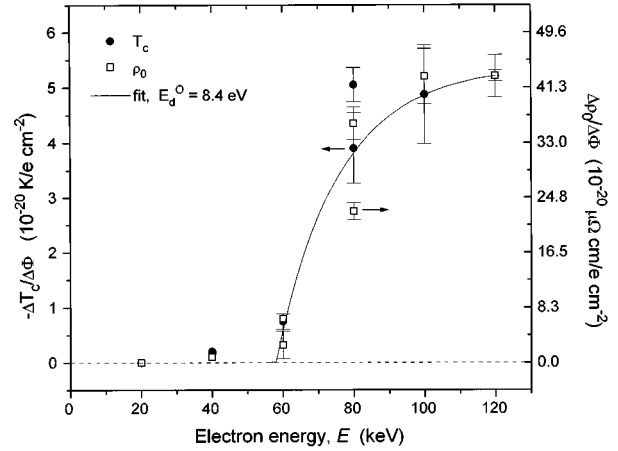


FIG. 7. Slopes ( $\Delta T_c/\Delta\Phi$ ) of  $T_c$ -vs- $\Phi$  dependences shown in Fig. 6 (left axis) and the slopes ( $\Delta\rho_0/\Delta\Phi$ ) of  $\rho_0$ -vs- $\Phi$  dependences (right axis) as a function of incident electron energy. The solid line is the best fit to the energy dependence of the Mott-Rutherford displacement cross section [Eq. (2)], giving  $E_d^O(\text{plane}) = 8.4 \pm 0.4$  eV.

low value of  $E_d^O$  is not specific to thin films. Independently of the thickness and fabrication method, the results were found to be consistent with the above value, which we believe, therefore, is appropriate also for bulk samples. Moreover, since CuO<sub>2</sub> planes in cuprate HTS's are all alike, we suggest that a plane oxygen displacement energy of 8.4 eV is also appropriate for other HTS materials. Preliminary results on low-energy electron irradiation of La<sub>2-x</sub>Sr<sub>x</sub>CuO<sub>4</sub> thin films confirm this suggestion.<sup>30</sup>

It is interesting to note that the low displacement energy of oxygen in YBCO follows also from molecular-dynamics simulation of radiation damage.<sup>31,32</sup> For instance, Cui *et al.*<sup>32</sup> found that  $E_d^O$  can be less than 9 eV for displacement of in-plane oxygen O(2) or O(3) into an interstitial site in the middle of two plane Cu(2) sites and about 4 eV for displacement of apical, O(4), oxygen to the O(5) site on the  $a$  axis.

#### D. Displacement energy for oxygen in chains

Let us now set the incident energy below the threshold for plane oxygen displacements and look at irradiation-induced changes in transport properties which can be associated with the formation of chain oxygen defects. The most noticeable feature of the resistivity data is the increase in  $\alpha$  with irradiation dose at unchanged (or slightly increasing)  $T_c$ , as shown in Fig. 8. It resembles an increase in  $\alpha$  that occurs in oxygen-deficient samples in the region of the 90-K plateau (see Fig. 2). We suggest that this increase in irradiated samples is primarily caused by chain disorder. Indeed, as known from the studies of detwinned single crystals,<sup>17,33</sup> the resistivity slope in the  $b$  direction,  $\alpha_b$ , is a factor of 2 smaller than the slope in the  $a$  directions,  $\alpha_a$ , in fully oxygenated samples due to the existence of an ordered CuO chain along the  $b$  axis and associated with it a band of carriers.<sup>34</sup> When  $x$  decreases,  $\alpha_b$  increases, approaching  $\alpha_a$  since oxygen removal decreases the effective length of chains. Similarly, if chains are being disordered at constant oxygen content, we expect an increase in  $\alpha_b$  and, corre-

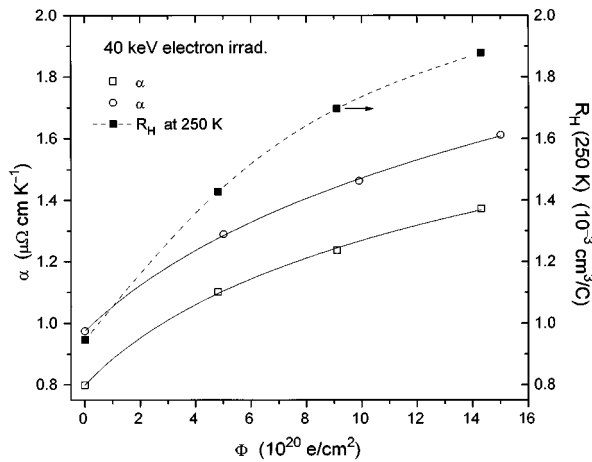


FIG. 8.  $T$ -linear resistivity slope (left axis) and Hall coefficient at 250 K (right axis) for two  $\text{YBa}_2\text{Cu}_3\text{O}_{6+x}$  ( $x \approx 0.9$ ) samples after different doses of 40-keV electron irradiation. ( $\square$ ), ( $\blacksquare$ ), sample No. TY43;  $T_c$  vs  $\Phi$  for this sample is shown in Fig. 6; ( $\circ$ ), sample No. TY44. Solid lines are fits to the athermal model.

spondingly, in  $ab$ -averaged slope in twinned samples. Chain disordering slightly decreases the carrier concentration and does not affect  $T_c$  if  $x$  is close to 1 as follows from the experiments with quenched oxygen-deficient samples.<sup>35</sup> Hall measurements do show an increase in  $R_H$  (decrease in  $n$ ?) in the irradiated samples in the same region of  $\Phi$  where  $\alpha$  increases (Fig. 8).

The effect of chain disorder on  $T_c$  is known to become more pronounced when  $x$  is far from the optimal doping, due to both a steeper dependence of  $T_c$  on  $n$  and  $n$  on the degree of ordering.<sup>35</sup> Indeed, at  $x=0.5$ , a complete chain disorder should result in a semiconducting phase,<sup>36</sup> while the formation of an ordered  $2 \times 1$  superstructure (ortho-II phase<sup>37</sup>) is known to lead to a 60-K superconducting phase. To illustrate the stronger influence of low-energy electron irradiation on  $T_c$  in oxygen-deficient samples, Fig. 9 shows the  $\rho$ -vs- $T$  curves of the oxygen-deficient sample before and after 40-keV electron irradiation. This energy is not sufficient to pro-

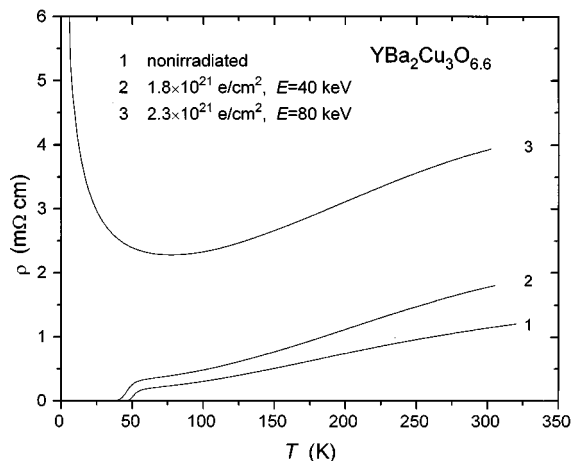


FIG. 9. In-plane resistivity of oxygen-deficient  $\text{YBa}_2\text{Cu}_3\text{O}_{6+x}$  ( $x \approx 0.6$ ) sample No. TY38 after irradiation with 40-keV and then 80-keV electrons.

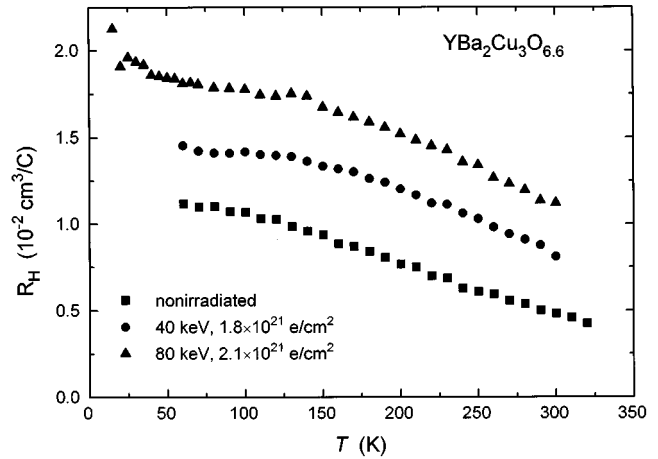


FIG. 10. Hall coefficient of the same sample as in Fig. 9.

duce in-plane defects, and only chain defects were apparently produced. As can be seen from these curves, there is a noticeable decrease in  $T_c$  and an increase in the resistivity slope, suggesting a decrease in carrier concentration. The Hall coefficient data presented in Fig. 10 support this suggestion.

While the influence of chain disordering on  $T_c$  in oxygen-deficient samples is noticeable, it is still small in comparison with the influence of in-plane oxygen defects. For example, about the same dose of 80-keV irradiation, capable of creating in-plane defects, completely destroys superconductivity as shown in Fig. 9; the conduction at low temperatures becomes a 2D variable-range hopping [ $\rho \sim \exp(T_0/T)^{1/3}$ ]. It is worth noticing that, despite the obvious effects of localization at low temperatures (which imply that the mean free path is extremely short), the temperature dependence of the resistivity at high temperatures (curve 3) has exactly the same form as in a low-residual-resistivity case (curve 2). The curves can be obtained from each other by a parallel shift along the  $\rho$  axis, corresponding to the suggested increase in the residual resistivity (Matthiessen's rule). Also, the magnitude of the resistivity (curve 3) at all temperatures exceeds the maximum metallic resistivity in two-dimensional systems (see below). These two facts do not fit into the framework of the conventional description of carrier transport in terms of the mean free path and propagating quasiparticles.<sup>16,38</sup>

At 20-keV irradiation (the lowest energy in the microscope), the observed changes are not much different from those found at 40 keV. So either 20 keV is still far from the threshold for chain oxygen displacements or the threshold does not exist. Taking 20 keV as the upper limit on  $E_c$ , we estimate the upper limit on  $E_d^O(\text{chains})$  as 2.8 eV. In a molecular-dynamics simulation of oxygen displacements from O(1) to O(5) sites, Cui *et al.*<sup>32</sup> found  $E_d^O$  to be as low as 1.5 eV, which is close to the oxygen diffusion activation energy of 1.3 eV. Another possibility is that the mechanism of chain disordering differs from knock-on. For instance, it can involve inelastic processes (ionization) similar to the mechanism of formation of  $F$  centers in alkali halides. Also, the energy barrier between the chain site and interstitial position on the  $a$  axis is low, and chain disordering can be induced by nonequilibrium phonons which are the final prod-



TABLE I. Initial rates of  $T_c$  suppression and residual resistivity increase by different in-plane defects in  $\text{YBa}_2\text{Cu}_3\text{O}_{6.9}$ .

Type of defects	$\delta T_c$ (K per defect cell <sup>-1</sup> )	$\delta\rho_0$ (m $\Omega$ cm per defect cell <sup>-1</sup> )	Comments
In-plane O defects (vacancies)	280	1.50	this work, $E=60-120$ keV
	274		$E=100$ keV, thin film <sup>a</sup>
	490		$E=350$ keV, single crystal <sup>b</sup>
Zn impurities	391	0.69	single crystals <sup>c</sup>
	410		single crystals <sup>d</sup>
	404		ceramics <sup>e</sup>
Ni impurities	190	3.3	thin films <sup>f</sup>
	140		thin films <sup>g</sup>
	60		ceramics <sup>e</sup>
	135		single crystals <sup>h</sup>

<sup>a</sup>Reference 6.

<sup>b</sup>Reference 7.

<sup>c</sup>Reference 19.

<sup>d</sup>Reference 22.

<sup>e</sup>Reference 54.

<sup>f</sup>Reference 43.

<sup>g</sup>Reference 44.

<sup>h</sup>Reference 55.

uct of energy release after any collision event. A low-energy tail in radiation damage rather than the threshold should be expected in these cases.

#### IV. DISCUSSION

##### A. Carrier scattering

Using the evaluated value of  $E_d^O$ , we can estimate the concentration of irradiation-induced defects and characterize quantitatively their effect on  $T_c$  and  $\rho_0$ . As above, we assume that the main contribution to  $T_c$  suppression and carrier scattering comes from the in-plane O vacancies. Their number per unit cell is given by Eq. (3) with  $N_O=4$  and  $\sigma_d$  from Eq. (2) at  $E_d^O=8.4$  eV. The values of  $\delta T_c$  and  $\delta\rho_0$  which characterize, respectively,  $T_c$  suppression and scattering strength of one defect in the low-concentration limit are given in Table I. The same set of parameters was used to extract these quantities from the data in Refs. 6 and 7. The  $\delta T_c$  shown agree quite well with the value extracted from the data by Legris *et al.*<sup>6</sup> taken at low incident electron energy. The higher-energy data in Refs. 6 and 7 imply somewhat bigger  $\delta T_c$ , which is probably due to the contribution of Cu displacements and secondary defect formation by primary knocked-on atoms. We have not tried to account for these processes, and so the  $\delta T_c$  value inferred from the data of Giapintzakis *et al.*<sup>7</sup> should be regarded as an upper limit on the actual  $\delta T_c$ . For a comparison, the corresponding values for Cu substitutions on Ni and Zn are also given. It was assumed that both atoms substitute only for plane Cu. As can be seen, the in-plane oxygen vacancies have an influence on  $T_c$  comparable with Zn impurities. It is interesting to note that there appears to be an anticorrelation of  $\delta T_c$  and  $\delta\rho_0$  for in-plane defects; i.e., the strongest  $T_c$  suppressors (Zn impurities) have the smallest effect on  $\rho_0$ . Also, for comparison,

vacancies in normal metals such as Cu increase the resistivity by  $\sim 1.5 \mu\Omega$  cm/at. %, which is some 50 times smaller than in YBCO.

Now we turn to the simplest model estimates with the obtained parameters. Since the carrier transport in YBCO is mainly of 2D character and there are two conducting planes in the unit cell, the resistivity in the Drude model can be expressed as  $\rho_0=(h/e^2k_F l_0)(c/2)$ , where  $h$  is the Planck's constant,  $c$  is the  $c$ -direction lattice constant,  $k_F$  is the Fermi wave vector, and  $l_0$  is the mean free path. According to the Ioffe-Regel criterion of metallic conduction, the shortest mean free path corresponds to  $k_F l_0 \sim 1$ ; i.e., for YBCO the maximum metallic resistivity is  $\rho_{\max}=hc/2e^2 \approx 1.5$  m $\Omega$  cm. From the data in Table I, we see that  $\rho_0$  in the irradiated samples would reach  $\rho_{\max}$  at  $N_v \approx 1$  cell<sup>-1</sup>, implying that  $k_F l_0 = 1$  at this defect concentration. At  $N_v = 1$  the mean distance between the defects in one plane is  $a$ , which in turn implies that  $k_F \approx 1/a$  (here  $a$  is the in-plane lattice constant, and we do not make a distinction between  $a$  and  $b$  since the orthorhombicity of YBCO is small). Band calculations, recent measurements of the Fermi surface, and various model calculations all suggest that  $k_F$  in  $\text{CuO}_2$  planes is about  $2.7/a$ .<sup>34,39,40</sup> Taking this value, the estimate of  $l_0$  at  $N_v \approx 1$  cell<sup>-1</sup> ( $\rho_0 \approx \rho_{\max}$ ) shows that the mean free path should be close to the length of the Cu-O bond, a reasonable figure. It will be shown below that superconductivity in optimally doped YBCO is completely suppressed at  $N_v \approx 0.2$  cell<sup>-1</sup>. At this concentration  $k_F l_0 \sim 5$  and  $l_0$  is about 7 Å; i.e., superconductivity in YBCO is destroyed when the impurity mean free path becomes shorter than the coherence length in defect-free material.

The defect-induced resistivity  $\rho_d$  can also be estimated using the expression for the transport impurity scattering cross section in 2D systems,<sup>41</sup>  $\sigma=(4/k_F)\sum \sin^2(\delta_l - \delta_{l+1})$ , which gives

$$\rho_d = (2\rho_{\max}n_d/k_F^2a^2) \sum_0^{\infty} \sin^2(\delta_l - \delta_{l+1}), \quad (7)$$

where we made use of the nearly square shape of the Fermi surface. Here  $\delta_l$  are the phase shifts of partial waves and  $n_d$  is the number of defects per unit cell. Phase shifts must satisfy a 2D analog of the Friedel sum rule,<sup>41</sup> which, for two plane bands, can be expressed as

$$(4/\pi) \sum_{-\infty}^{\infty} \delta_l = Q. \quad (8)$$

The effective charge of a defect,  $Q$ , is determined by the valence difference of the host atom and defect,  $Q_1$ , as well as by a change in the local ionic charge density resulting from the distortion of the unit cell occupied by the defect,  $Q_2$ .<sup>42</sup> Since  $\text{Zn}^{2+}$  ions substitute for  $\text{Cu}^{2+}$  ions,  $Q_1$  is formally zero for Zn impurities;  $Q_2$  we estimated as  $-0.15$ . However, the replacement of Cu by Zn reduces the number of  $3d$  holes in plane bands by 1. Therefore, it seems reasonable that  $Q_1$  should be taken as  $+1$ , and consequently  $Q_{\text{Zn}}$  becomes  $0.85$ . It is also likely that  $s$ - and  $p$ -wave shifts would dominate at scattering off Zn impurities. Indeed, in the  $s$ -wave unitary limit, we obtain from Eq. (7) that  $\Delta\rho_0 \equiv \rho_d/n_d$  is  $0.41$  m $\Omega$  cm per defect, which is in fair agreement with the contribution of Zn impurities (see Table I). For the in-plane oxygen vacancies,  $Q_v$  is about  $+2$ , and we expect that  $p$ - and  $d$ -wave shifts should dominate. The Ni impurity increases the number of  $d$  holes by 1, and  $Q_{\text{Ni}}$  should probably be taken as close to  $-1$ . The effect of Ni impurities on  $\rho_0$  should be regarded as enormously strong, if the resistivity data we used<sup>43,44</sup> were not affected by a change in the microstructure of Ni-doped films with respect to undoped ones. Indeed, even if we take all the  $s$ ,  $p$ ,  $d$ , and  $f$  shifts such as to maximize the sum in Eq. (7), i.e.,  $\sin^2(\delta_l - \delta_{l+1}) = 1$  for  $l \leq 3$ , the calculated  $\Delta\rho_0$  is still a factor of 2 smaller than the Ni contribution suggested by thin-film data.<sup>43,44</sup> Note, however, that optical measurements on the same films suggest considerably smaller  $\rho_0$  than do the resistivity data,<sup>44</sup> which would be a plausible resolution. Recent data on Ni-doped single crystals<sup>55</sup> also show much lower resistivities and  $\delta\rho_0$  which are close to those in Zn-doped crystals.

The transport scattering cross section of in-plane oxygen vacancies can be represented by a disk, diameter  $\sigma_{\text{tr}}$ , and can be estimated from Eq. (7), which is equivalent to the expression  $\rho_d = (\hbar c/2e^2)(n_d/n)(k_F\sigma_{\text{tr}})$ . If we take the hole concentration  $n = 0.34$  cell<sup>-1</sup>, which follows from bond valence sums and charge transfer models, it results in  $k_F\sigma_{\text{tr}} = 2.13$  and, if the band value of  $k_F$  is used, a scattering diameter of  $3$  Å. From the  $T_c$  suppression rate shown in Table I, the critical concentration of vacancies which brings  $T_c$  down to zero is about  $0.3$  cell<sup>-1</sup>. More detailed consideration based on pair-breaking theory (see below) suggests the critical concentration to be  $0.2$  cell<sup>-1</sup>. Since the O-O distance in planes is  $a/\sqrt{2}$ , the mean separation of vacancies in one plane at this defect concentration is about  $9$  Å and is considerably larger than  $\sigma_{\text{tr}}$ , which to some extent justifies our treatment of scattering centers and scattering events as completely independent.

The transport impurity scattering rate in the Drude model is  $1/\tau_{\text{imp}} = \rho_0\omega_p^2/4\pi$ . Using the generally accepted value of

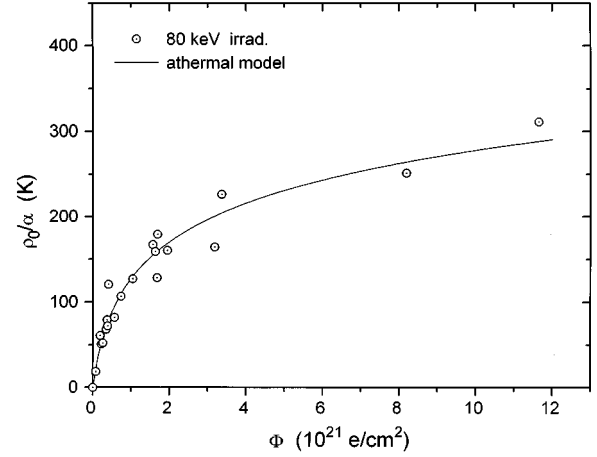


FIG. 11.  $\rho_0/\alpha$  for  $x \approx 0.9$  YBCO samples vs irradiation fluence of 80-keV electron irradiation. The solid line is the best fit to the athermal model [Eq. (9)] at  $v_r = 21$  and  $\delta\tau^{-1} = 3.7 \times 10^{14}$  s<sup>-1</sup> per oxygen defect in the unit cell.

the plasma frequency in  $\text{YBa}_2\text{Cu}_3\text{O}_{6.9}$ ,  $\hbar\omega_p = 1.1$  eV, for the scattering rate off in-plane oxygen vacancies, we obtain  $\delta\tau^{-1} = 3.5 \times 10^{14}$  s<sup>-1</sup> per defect in the unit cell, where  $\delta\tau^{-1} \equiv \tau_{\text{imp}}^{-1}/N_v$ .

We would like to note here that  $\rho_0$  is not always a good measure of impurity scattering in HTS samples, especially if it is necessary to compare samples of different quality, because the value of  $\rho_0$  can be affected by the microstructure of the samples (grain boundaries, twins, etc.). Also, even at modest concentrations, point defects can aggregate, forming poorly conducting regions, and so the actual length of the current path can be greater than that suggested by sample geometry. Analyzing a great deal of our own and published data, we have found that the quantity  $\rho_0/\alpha$  ( $\alpha$  is taken in the  $T$ -linear resistivity region) provides a better representation of the actual impurity scattering. Indeed, the effect of macroscopic inhomogeneities and uncertainty in the dimensions of samples on the length of the current path equally affects both  $\alpha$  and  $\rho_0$  and, therefore, cancels in  $\rho_0/\alpha$ . While  $\rho_0$  depends on the carrier concentration, which can be different even in nominally identical samples, e.g., due to variations in oxygen content, this dependence also cancels in  $\rho_0/\alpha$ . So  $\rho_0/\alpha$  better represents scattering off point defects than  $\rho_0$  alone. In the Drude model, the relation with impurity scattering rate is  $\rho_0/\alpha = \tau_{\text{imp}}^{-1}/2\pi\lambda_{\text{tr}}$ ;  $\lambda_{\text{tr}}$  is more or less well known for oxygenated YBCO and according to various estimates is about  $0.3$ .<sup>45</sup>

Figure 11 shows  $\rho_0/\alpha$  for the irradiated films as a function of irradiation dose. In the athermal model, we obtain

$$\rho_0/\alpha = \frac{\delta\tau^{-1}}{2\pi\lambda_{\text{tr}}v_r} \ln(4\sigma_d v_r \Phi + 1). \quad (9)$$

Using the same parameter values  $\sigma_d = 6.09 \times 10^{-23}$  cm<sup>2</sup> and  $v_r = 21$  as before (see the fit in Fig. 5) and taking  $\lambda_{\text{tr}} = 0.3$ , the fit to the data in Fig. 11 gives  $\delta\tau^{-1} = 3.7 \times 10^{14}$  s<sup>-1</sup>/defect, in good agreement with the value evaluated from  $\rho_0$ . Using  $\rho_0/\alpha$  inferred from the resistivity curves for Zn-doped single crystals in Ref. 19, we obtained  $\delta\tau_{\text{Zn}}^{-1} = 3.1 \times 10^{14}$  s<sup>-1</sup> per Zn atom, a value close to the scattering rate off oxygen vacan-

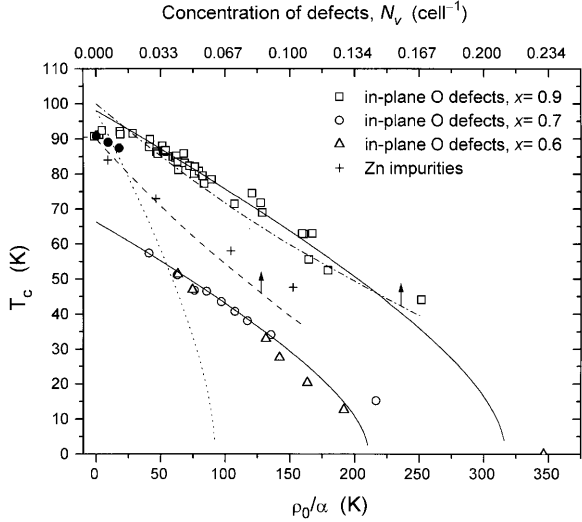


FIG. 12. Critical temperature of  $\text{YBa}_2\text{Cu}_3\text{O}_{6+x}$  samples with in-plane oxygen defects (vacancies) induced by 60–120 keV electron irradiation vs  $\rho_0/\alpha = 1/2\pi\lambda_{\text{tr}}\tau_{\text{imp}}$ . The upper scale shows the evaluated concentration of in-plane oxygen vacancies and is applicable to the irradiated samples, dashed and dash-dotted curves. Also the data are shown for Zn-doped single crystals (+) extracted from Ref. 19 and for 350-keV electron-irradiated detwinned single crystal (●) from Ref. 7. The dotted curve is the prediction for  $T_c$  suppression in  $\text{YBa}_2\text{Cu}_3\text{O}_{6.9}$  of pair-breaking theory for  $d$ -wave pairing; Eq. (10) at  $\hbar\omega_p = 1.1$  eV ( $\lambda_{\text{tr}} = 0.3$ ) and  $\tau_p = \tau_{\text{imp}}$ . Solid lines are the best fits to pair-breaking theory for  $d$ -wave pairing and  $\lambda_{\text{tr}} = 0.3$ , giving  $\tau_p^{-1} = 0.29\tau_{\text{imp}}^{-1}$ . The suggested  $T_{c0}$  is 98 and 67 K for  $x = 0.9$  and  $0.7$ , respectively. Dashed and dash-dotted curves show the defect-induced  $T_c$  suppression at different strengths of potential impurity scattering according to a strong-coupling calculation by Monthoux and Pines (Ref. 2) for spin-fluctuation-mediated superconductivity; dashed curve,  $T_{c0} = 90$  K,  $V = 2.5$  eV; dash-dotted curve,  $T_{c0} = 100$  K,  $V = 0.5$  eV.

cies, but a factor of 2 higher than the value given in Ref. 19 and which follows from the  $\delta\rho_0$  in Table I.

### B. $T_c$ suppression

As follows from Sec. III, the determination of the exact concentration of radiation defects is extremely complex. For substitutions it is also not trivial because substitution probabilities on different sublattices in HTS's are not exactly known. Therefore, in this section we will use the quantity  $\rho_0/\alpha$  in order to characterize the *integral effect of all the defects* induced by irradiation or substitution and retained in the samples up to the moment of  $T_c$  measurements, including also possible effect of induced lattice strains, etc.

In Fig. 12 we plotted  $T_c$  as a function of  $\rho_0/\alpha$  (i.e.,  $\tau_{\text{imp}}^{-1}$ ) for all the samples studied. The upper scale shows our best estimate of the concentration of in-plane oxygen defects. Also shown are the data for Zn-doped samples<sup>19</sup> and an irradiated detwinned single crystal.<sup>7</sup> If we disregard the plateaulike region at small  $\rho_0/\alpha$ , which, as explained above, arises from superposition of the effects of plane and chain defects, it is seen that the rate of  $T_c$  suppression in the irradiated thin films, irradiated single crystal, and in Zn-doped crystals is almost identical. This suggests a universal mechanism of  $T_c$  suppression by in-plane defects, which is also

independent of (or only weakly depends on) carrier concentration as follows from our data on irradiated oxygen-deficient samples (Fig. 12). In our work<sup>46</sup> we have shown that this universal behavior can be explained in the framework of standard pair-breaking theory (see also Refs. 23, 47, and 48). Two cases have been considered. These are pair breaking due to potential impurity scattering in anisotropic (e.g.,  $d$ -wave) superconductors and spin-flip scattering off magnetic impurities in isotropic superconductors. There have been many arguments and some evidence in support of the nonmagnetic nature of in-plane oxygen vacancies. Therefore, we consider in brief only the former case. The well-known expression for the  $T_c$  in anisotropic superconductors in the presence of impurity scattering is<sup>49–51</sup>

$$\ln \frac{T_{c0}}{T_c} = \chi \left[ \psi \left( \frac{1}{2} + \frac{1}{4\pi T_c \tau_p} \right) - \psi \left( \frac{1}{2} \right) \right], \quad (10)$$

where  $T_{c0}$  is the critical temperature of pair-breaking-free material,  $\psi$  is the digamma function,  $\chi$  is the anisotropy parameter, and  $\tau_p$  is the pair-breaking scattering time. In the case of  $d$ -wave pairing,  $\tau_p$  is usually identified with the impurity scattering time  $\tau$  (the symbol  $\tau_{\text{imp}}$  was reserved for the transport scattering time). The former can be expressed as<sup>52</sup>

$$h/\tau = 4n_d z^2/N(0)(1+z^2), \quad (11)$$

where  $z \equiv \pi N(0)V$ ,  $N(0)$  is the density of states, and  $V$  is the scattering potential. At a small concentration of defects, Eq. (10) reduces to

$$\Delta T_c \equiv T_{c0} - T_c = \chi h/16k_B\tau. \quad (12)$$

It was argued earlier<sup>23,46</sup> that the data on irradiation-induced  $T_c$  suppression suggest that  $\chi$  in HTS's is close to 1. From the data in Fig. 12, the lower limit on  $\chi$  can be estimated as 0.8.<sup>53</sup> Therefore, for definiteness, we consider  $d$ -wave pairing and set  $\chi = 1$ . From  $\delta T_c$  given in Table I and Eqs. (11) and (12), we estimate the scattering potential of oxygen vacancies as  $N(0)V_O = 0.11$ . If we take the density of states associated with two  $\text{CuO}_2$  planes from the band calculations<sup>34</sup> as 1.1 states  $\text{eV}^{-1}$  per spin cell, then  $V_O$  required to fit the data to pair-breaking theory is 0.10 eV cell (see also Refs. 23 and 47). This seems to be too small a figure because in normal metals the scattering potentials of impurities are usually about the Fermi energy  $E_F$  or bandwidth, and  $E_F$  in YBCO is  $\sim 0.3$  eV. It also appears to be too small to account for the strong effect of oxygen defects on the resistivity. Indeed, neglecting a subtle difference between transport and scattering lifetime, using (11), and the scattering rate per oxygen defect estimated above, we estimate  $N(0)V_O$  as 0.27 and, correspondingly,  $V_O$  as 0.25 eV cell, which is closer to the generally assumed Fermi energy. Unfortunately, we do not have any possibility of direct measurement or evaluation of  $V_O$  from independent experiments.

In order to compare defect-induced  $T_c$  suppression with pair-breaking theory, Millis *et al.*<sup>49</sup> and Radtke *et al.*<sup>51</sup> suggested the use in Eq. (10) of a transport impurity scattering rate which can be inferred from the resistivity using either experimentally determined values of  $\omega_p$  or  $\lambda_{\text{tr}}$ . If we do so, pair-breaking theory, Eq. (10), predicts a factor of 3 faster  $T_c$  suppression (dotted curve in Fig. 12) than that observed (see also Refs. 47 and 48). Formal fitting the data to pair-breaking

theory for  $d$ -wave superconductors requires  $\lambda_{tr}$  to be 0.092 or  $\omega_p = 0.61$  eV. In other words, to be consistent with the data, the pair-breaking scattering rate in YBCO should be  $\approx 0.29\tau_{imp}^{-1}$ , independent of the carrier concentration (see Fig. 12, solid curves). A possible rationale for this reduction, such as scattering anisotropy and/or strong-coupling corrections, was discussed elsewhere.<sup>7,46</sup>

The fitting to pair-breaking theory also suggests that the critical temperature in an ideal YBCO sample with the optimal oxygen content,  $T_{c0}$ , may be as high as 98 K, which is about 5 K higher than the critical temperature reported for the best single crystals. It is interesting to note that this difference corresponds almost exactly to the possible  $T_c$  reduction in optimally doped YBCO because of quantum phase fluctuations as shown by Emery and Kivelson.<sup>38</sup>

The arguments against treating the scattering in the  $\tau$  approximation were given by Monthoux and Pines<sup>2</sup> who presented numerical calculations of  $T_c$  suppression which take into account the specific nature of the quasiparticle spectrum and spin fluctuations in HTS's. Their results for isotropic potential impurity scattering of different strengths and values of  $T_{c0}$  are shown in Fig. 12. It is seen that the data can be described in the MP model quite well. It is worth mentioning that  $T_c$  suppression by Zn impurities can also be described as due to potential scattering, and there may be no need for the additional mechanism suggested by MP, which involves suppression of spin fluctuations around Zn atoms.

## V. SUMMARY

To summarize, we have studied the effects of electron irradiation with energy from 20 to 120 keV on the resistivity, Hall coefficient, and superconducting critical temperature of  $\text{YBa}_2\text{Cu}_3\text{O}_{6+x}$  ( $x=0.9$  and  $0.7$ ) thin films. By analyzing the changes in properties at different energies of incident electrons, we have found the threshold energy for displacement of oxygen on  $\text{CuO}_2$  planes and evaluated the displacement energy for plane oxygen as 8.4 eV. We have also studied the kinetics of accumulation of oxygen defects at electron irradiation and found that this kinetics is governed by athermal recombination of vacancy-interstitial pairs. Using  $T_c$ -vs- $\Phi$  and  $\rho$ -vs- $\Phi$  dependences at energies above the threshold and evaluated displacement energy and cross section, we estimated the volume of instability (recombination volume) of vacancy-interstitial pairs as 21 unit cells. Also, assuming that only oxygen vacancies on planes are responsible for the irradiation-induced  $T_c$  suppression and increase in the residual resistivity, we have evaluated their effect on resistivity as 1.5 m $\Omega$  cm per vacancy in the unit cell and their effect on  $T_c$  as  $-280$  K per vacancy in the unit cell. The carrier scattering rate was evaluated as  $(3.5-3.7)\times 10^{14}$  s<sup>-1</sup> per oxygen defect.

Analyzing the dependence of  $T_c$  on the irradiation-induced resistivity (impurity scattering rate) in a wide range of oxygen defect concentrations in planes and in samples with different oxygen contents, we have shown that  $T_c$  suppression is qualitatively consistent with the pair-breaking theory for  $d$ -wave superconductors. The obtained data have constrained the minimum value of the order parameter anisotropy  $\chi$  by 0.8. A quantitative description of the data in  $d$ -wave pair-breaking theory requires that the pair-breaking

scattering rate be at least a factor of 3 smaller than the transport impurity scattering rate. We have also shown that  $T_c$  suppression by in-plane oxygen defects is comparable to that by Zn substitutions for plane Cu. In both cases the  $T_c$  suppression was found to be in agreement with strong-coupling numerical calculations by Monthoux and Pines for the effect of potential impurity scattering on  $T_c$  in the framework of the nearly antiferromagnetic Fermi-liquid model of HTS's.

In irradiations with electron energy below the threshold for displacement of plane oxygen, we have observed an increase in the  $T$ -linear resistivity slope and Hall coefficient, and ascribed it to the effect of chain oxygen displacements. The upper limit on the displacement energy for chain oxygen was estimated as 2.8 eV. It was also found that irradiation in the 20–40 keV energy range slightly increases  $T_c$  in fully oxygenated samples, but decreases  $T_c$  in oxygen-deficient samples. More detailed results will be published elsewhere. Also, an interesting phenomenon we have only mentioned in this paper is a stretched exponential relaxation (aging) of irradiation-induced changes in  $T_c$  and resistivity, which closely resembles magnetic and dielectric relaxation in glasses. This subject deserves, however, a separate publication.<sup>24</sup>

In conclusion, we would like to list some of the phenomena in HTS's in which oxygen in-plane defects may play an important role due to their strong influence on  $T_c$ . For example, a well-known  $T_c$  suppression near the grain boundaries as well as the dependence of Josephson properties of grain boundary junctions on misorientation angle could to a large extent be explained by the presence of oxygen vacancies and/or oxygen atoms with broken bonds or locally distorted coordination. The influence of such defects should be much stronger than that of possible nonuniform distribution and/or reduction of oxygen content in chains, which is usually invoked in discussions of transport across grain boundaries in HTS's. Also, since vacancies are defects in thermal equilibrium and at high temperatures their concentration in planes can reach several percent, it would be interesting to clarify whether they contribute to  $T_c$  suppression in quenched samples. Undoubtedly, the effects of in-plane oxygen defects studied in this work govern the Josephson properties of weak links and flux-flow devices created in HTS thin films by focused electron-beam writing<sup>8,12,56</sup> as well as by focused ion irradiation. And finally, realizing the importance of in-plane oxygen defects, one can even make a suggestion that these defects might be forming as a result of substitution for plane copper and therefore might be partially responsible for the changes in properties of samples doped on the Cu sublattice as well.

## ACKNOWLEDGMENTS

We are very grateful to B. Nadgorny and S. Shokhor with whom we discussed this work from its earliest stage and for their help with *in situ* resistivity measurements. Early discussions with A. Bourdillon are also appreciated. We would like to thank J. Lukens and M. Bhushan for access to microfabrication facilities, and A. King for access to the electron microscope used in this work. Some of the films tested in the course of this work were fabricated and kindly given to us by D. Rudman, R. Ono, Qi Li, and P. Rosenthal. This work was supported by Grant No. N000149510762 sponsored by the U.S. Office of Naval Research, and by BNL Project No. 737151.

- \*Present address: Sandia National Laboratories, Albuquerque, NM 87185
- <sup>1</sup>For a review of early work, see, e.g., J. T. Market, Y. Dalichaouch, and M. B. Maple, in *Physical Properties of High-Temperature Superconductors I*, edited by D. M. Ginsberg (World Scientific, New York, 1990), p. 265; L. H. Greene and B. H. Bagley, in *Physical Properties of High-Temperature Superconductors II*, edited by D. M. Ginsberg (World Scientific, New York, 1990), p. 509.
  - <sup>2</sup>P. Monthoux and D. Pines, *Phys. Rev. B* **49**, 4261 (1994).
  - <sup>3</sup>P. Monthoux, A. Balatsky, and D. Pines, *Phys. Rev. B* **46**, 14 803 (1992); P. Monthoux and D. Pines, *ibid.* **47**, 6069 (1993).
  - <sup>4</sup>For a review, see M. A. Kirk, in *Defects in Materials*, edited by P. D. Bristowe, J. E. Epperson, J. E. Griffith, and Z. Liliental-Weber, MRS Symposia Proceedings No. 209 (Materials Research Society, Pittsburgh, 1991), p. 743.
  - <sup>5</sup>G. P. Summers *et al.*, *Appl. Phys. Lett.* **55**, 1469 (1989); B. D. Weaver, E. M. Jackson, G. P. Summers, and E. A. Burke, *Phys. Rev. B* **46**, 1134 (1992), and references therein.
  - <sup>6</sup>A. Legris, F. Rullier-Albenque, E. Radeva, and P. Lejay, *J. Phys. (France)* **3**, 1605 (1993).
  - <sup>7</sup>J. Giapintzakis, D. M. Ginsberg, M. A. Kirk, and S. Ockers, *Phys. Rev. B* **50**, 15 967 (1994).
  - <sup>8</sup>S. K. Tolpygo *et al.*, *IEEE Trans. Appl. Supercond.* **AS-5**, 2521 (1995).
  - <sup>9</sup>For a review, see C. Lehmann, *Interaction of Radiation with Solids and Elementary Defect Production* (North-Holland, Amsterdam, 1977).
  - <sup>10</sup>F. Seitz and J. S. Koehler, in *Solid State Physics*, edited by F. Seitz and D. Turnbull (Academic, New York, 1956), Vol. 2.
  - <sup>11</sup>S. N. Basu, T. E. Mitchell, and M. Nastasi, *J. Appl. Phys.* **69**, 3167 (1991).
  - <sup>12</sup>S. K. Tolpygo *et al.*, *Physica C* **209**, 211 (1993); S. K. Tolpygo *et al.*, *Appl. Phys. Lett.* **63**, 1696 (1993); J. M. Macaulay *et al.*, *Superlatt. Microstruct.* **11**, 211 (1992), and references therein.
  - <sup>13</sup>M. P. Siegal *et al.*, *J. Mater. Res.* **7**, 2658 (1992).
  - <sup>14</sup>For a review, see F. W. Clinard and L. W. Hobbs, in *Physics of Irradiation Effects in Crystals*, edited by R. A. Johnson and A. N. Orlov (North-Holland, Amsterdam, 1986), p. 387.
  - <sup>15</sup>See, e.g., B. Batlogg, in *High Temperature Superconductivity: Proceedings*, edited by K. S. Bedell, D. Coffey, D. E. Meltzer, D. Pines, and J. R. Shriver (Addison-Wesley, Redwood City, CA, 1990), p. 37.
  - <sup>16</sup>For a discussion, see P. B. Allen, *Comments Condens. Matter Phys.* **15**, 327 (1992), and Ref. 38.
  - <sup>17</sup>T. Ito, K. Takenaka, and S. Uchida, *Phys. Rev. Lett.* **70**, 3995 (1993).
  - <sup>18</sup>E. C. Jones *et al.*, *Phys. Rev. B* **47**, 8986 (1993).
  - <sup>19</sup>T. R. Chien, Z. Z. Wang, and N. P. Ong, *Phys. Rev. Lett.* **67**, 2088 (1991).
  - <sup>20</sup>A. Carrington, D. J. C. Walker, A. P. Mackenzie, and J. R. Cooper, *Phys. Rev. B* **48**, 13 051 (1993).
  - <sup>21</sup>B. Wuyts *et al.*, *Physica C* **222**, 341 (1994).
  - <sup>22</sup>K. Mizuhashi *et al.*, *Phys. Rev. B* **52**, R3884 (1995).
  - <sup>23</sup>E. M. Jackson *et al.*, *Phys. Rev. Lett.* **74**, 3033 (1995).
  - <sup>24</sup>S. K. Tolpygo *et al.* (unpublished).
  - <sup>25</sup>H. J. Wollenberger, in *Vacancies and Interstitial in Metals*, edited by A. Seeger, D. Schuhmacher, W. Seehling, and J. Diehl (North-Holland, Amsterdam, 1970), p. 215.
  - <sup>26</sup>A. E. Hughes and D. Pooley, *J. Phys. C* **4**, 1963 (1971), and references therein.
  - <sup>27</sup>See the curve for  $E=40$  keV in Fig. 6, and S. K. Tolpygo, J.-Y. Lin, and M. Gurvitch (unpublished).
  - <sup>28</sup>H. Cluas *et al.*, *Physica C* **198**, 42 (1992).
  - <sup>29</sup>R. Feenstra, D. K. Christen, C. E. Klabune, and J. D. Budai, *Phys. Rev. B* **45**, 7555 (1992); V. Matijasevic *et al.*, *J. Mater. Res.* **6**, 682 (1991).
  - <sup>30</sup>B. Nadgorny (private communication).
  - <sup>31</sup>V. V. Kirsanov and N. N. Musin, *Phys. Lett. A* **153**, 493 (1991).
  - <sup>32</sup>F. Z. Cui, J. Xie, and H. D. Li, *Phys. Rev. B* **46**, 11 182 (1992).
  - <sup>33</sup>K. Takenaka, K. Mizuhashi, H. Takagi, and S. Uchida, *Phys. Rev. B* **50**, 6534 (1994).
  - <sup>34</sup>W. E. Pickett, *Rev. Mod. Phys.* **61**, 433 (1989).
  - <sup>35</sup>B. W. Veal *et al.*, *Phys. Rev. B* **42**, 6305 (1990).
  - <sup>36</sup>R. P. Gupta and M. Gupta, *Phys. Rev. B* **44**, 2739 (1991).
  - <sup>37</sup>See, e.g., R. McComack, D. de Fontaine, and G. Ceder, *Phys. Rev. B* **45**, 12 976 (1991), and references therein.
  - <sup>38</sup>V. J. Emery and S. A. Kivelson, *Phys. Rev. Lett.* **47**, 3253 (1995).
  - <sup>39</sup>R. Liu *et al.*, *Phys. Rev. B* **46**, 11 056 (1992).
  - <sup>40</sup>Q. Si, Y. Zha, K. Levin, and J. P. Lu, *Phys. Rev. B* **47**, 9055 (1993).
  - <sup>41</sup>F. Stern and W. E. Howard, *Phys. Rev.* **163**, 816 (1967).
  - <sup>42</sup>F. J. Blatt, *Phys. Rev.* **108**, 285 (1957).
  - <sup>43</sup>J.-T. Kim, D. G. Xenikos, A. Thorns, and T. R. Lemberger, *J. Appl. Phys.* **72**, 803 (1992).
  - <sup>44</sup>M. J. Sumner, J.-T. Kim, and T. R. Lemberger, *Phys. Rev. B* **47**, 12 248 (1993).
  - <sup>45</sup>M. Gurvitch and A. T. Fiory, *Phys. Rev. Lett.* **59**, 1337 (1987).
  - <sup>46</sup>S. K. Tolpygo *et al.*, preceding paper, *Phys. Rev. B* **53**, 12 454 (1996).
  - <sup>47</sup>S. K. Tolpygo, *Phys. Rev. Lett.* **75**, 3197 (1995).
  - <sup>48</sup>P. Monod, K. Maki, and F. Rullier-Albenque, *Phys. Rev. Lett.* **75**, 3198 (1995).
  - <sup>49</sup>A. J. Millis, S. Sachdev, and C. M. Varma, *Phys. Rev. B* **37**, 4975 (1988).
  - <sup>50</sup>A. A. Abrikosov, *Physica C* **214**, 107 (1993).
  - <sup>51</sup>R. J. Radtke, K. Levin, H.-B. Shüttler, and M. R. Norman, *Phys. Rev. B* **48**, 653 (1993).
  - <sup>52</sup>See, e.g., H. Kim, G. Prelsti, and P. Muzikar, *Phys. Rev. B* **49**, 3544 (1994).
  - <sup>53</sup>J.-Y. Lin, Ph.D. thesis, State University of New York at Stony Brook, 1995.
  - <sup>54</sup>K. Ishida *et al.*, *J. Phys. Soc. Jpn.* **62**, 2803 (1993).
  - <sup>55</sup>J.-T. Kim, J. Giapintzakis, and D. M. Ginsberg, *Phys. Rev. B* **53**, 5922 (1996).
  - <sup>56</sup>A. J. Pauza *et al.*, *IEEE Trans. Appl. Supercond.* **AS-3**, 2405 (1993), and references therein.